Environmental Monitoring and Assessment (2005) **105:** 25–42
DOI: 10.1007/s10661-005-2815-x

GEOSTATISTICAL UNCERTAINTY MODELLING FOR THE ENVIRONMENTAL HAZARD ASSESSMENT DURING SINGLE EROSIVE RAINSTORM EVENTS

NAZZARENO DIODATO
Research Observatory on Climate and Landscape-ROC&L, Contrada Monte Pino, 82100 Benevento, Italy
(e-mail: nazdiod@tin.it)

(Received 18 January 2004; accepted 21 June 2004)

Abstract. This paper presents an environmental hazard assessment to account the impacts of single rainstorm variability on river-torrential landscape identified as potentially vulnerable mainly to erosional soil degradation processes. An algorithm for the characterisation of this impact, called Erosive Hazard Index (EHI), is developed with a less expensive methodology. In EHI modelling, we assume that the river-torrential system has adapted to the natural hydrological regime, and a sudden fluctuation in this regime, especially those exceeding thresholds for an acceptable range of flexibility, may have disastrous consequences for the mountain environment. The hazard analysis links key rainstorm energy variables expressed as a single-storm erosion index (EI_{sto}), with impact thresholds identified using an intensity pattern model. Afterwards, the conditional probabilities of exceeding these thresholds are spatially assessed using non-parametric geostatistical techinques, known as indicator kriging. The approach was applied to a test site in river-torrential landscape of the Southern Italy (Benevento province) for 13 November 1997 rainstorm event.

Keywords: rainstorm, soil erosion, hazard mapping, geostatistical, GIS, Benevento (Southern Italy)

1. Introduction

Land degradation by stormwater is perceived as one of the main problems worldwide since land degradation implies a large environmental and economic impact in agricultural areas (Cooke and Doornkamp, 1990; Ramírez and Finnerty, 1996; Lal, 1997; Steer, 1998; Arshad and Martin, 2002) and in river-torrential areas (Thornes and Alcántara-Ayala, 1998; Camarasa Belmonte and Segura Beltrán, 2001; Singh and Sen Roy, 2002). This is particularly so in areas such as Mediterranean Europe, which is subject to cyclical fluctuations in precipitation and drought periods associated with wildland fire (Bryant, 1991; Morgan, 1995; De Luís *et al.*, 2001; Conedera *et al.*, 2003; Ramos and Mulligan, 2003).

The spatial–time variability of weather, especially rainfall, is extremely important for soil erosion risk assessment (Renschler *et al.*, 1999; Le Bissonnais *et al.*, 2002). Such indicators of rainfall erosive potential (see Jansson 1982; Mikhailova *et al.*, 1997; Mati *et al.*, 2000; Krishnaswamy *et al.*, 2001) or application of soil erosion assessment tools (after Mitasova *et al.*, 1996; Abel *et al.*, 2000; van der Knijff, 2000; Lin *et al.*, 2002; Shi *et al.*, 2002), as well as design of soil conservation management and control of erosion (Al-Sheriadeh and Al-harndan, 1997; Cox and Madramootoo, 1998) are based on long-term average precipitation patterns. However, soil losses and geomorphologic processes are often dominated by a few severe storms (Larson *et al.*, 1997; Mulligan, 1998; Renschler and Harbor, 2002), within rainfall pattern exhibiting wide range of spatial variability (Mazzarella *et al.*, 1999; Hooke and Mant, 2000; Gardner and Gerrard, 2003).

Rainstorms are very significant for soil hydrology in river-torrential environments and croplands, which tend to provoke high-magnitude geomorphological processes and disastrous consequences in soil losses degradation, as in recent examples of Vaison La-Romaine (SE France) with 34 Mg ha^{-1} on 22 September 1992 (Wainwright, 1996), of the Era valley (Toscana, Italy) with 130 Mg ha^{-1} on March 1995 (Bazzoffi *et al.*, 1997), of Ronco s./Ascona (Ticino, Switzerland) with 127 Mg ha^{-1} on 28 August 1997 (Conedera *et al.*, 2003), of the Rio Camacho (Southern Bolivia) with 150 Mg ha^{-1} on 28 November 1999 (Coppus and Imeson, 2002), of Alt-Penedès-Anoia (Catalonia, Spain) with 207 Mg ha^{-1} on 10 June 2000 (Martínez-Casasnovas *et al.*, 2002).

During the past few decades there have been by many severe episodes of extreme events, probably connected to climate change (Trenberth, 1999; Balling Jr and Cerveny, 2003; Bell *et al.*, 2004). So that, several research studies have demonstrated increasing trends in these extreme hydrometeorological phenomena: for Northeastern Italy, in agreement with a reduction in return period for extreme rainfall (Brunetti *et al.*, 2001), for Portugal (de Santos Loureiro and Azevedo Coutinho, 1995) and for Southern Italy Apennines (Diodato, 2004a), in order an increase in rainfall erosivity. These results were confirmed by Alpert *et al.* (2002) who analysed the torrential rainfall for all of Italy during 1951–1995, detecting that rainfall increased percentage-wise by a factor of 4 with strong peaks El-Nino years.

Although distribution of extreme hydrometeorological events operates on a global and regional scale, they may be exacerbated from sub-regional processes operating at different spatial scales (Molnar *et al.*, 2002). Therefore, assessment of the rainstorm-induced geomorphological hazard should be performed and mapped at a locale scale, where land use can influence the flexibility and capability ecosystems of absorbing stresses caused by various forms of disturbance, including erosional soil degradation (Evans, 1993; De Luís *et al.*, 2001; Ferrero *et al.*, 2002; Mendoza *et al.*, 2002). Scale is a critical issue in soil erosion modelling and policy because it influences model development, as well as data availability and quality (Renschler and Harbor, 2002). Traditional isoerodent maps have been commonly used as an useful tool to estimate erosion indices at local, regional or national scale. However, they are not suitable to assess erosive rainfall hazard and are not useful to define the most appropriate change of spatial scales.

Alternative approaches, such as stochastic methods, was made by Goovaerts (1999) using multivariate extensions of kriging, and by Wang *et al.* (2002) employing the sequential Gaussian simulation algorithm, or like approach efficient for extreme rainfall (Atkinson and Lloyd, 1998; Prudhomme and Reed, 1999; Cheng *et al*., 2003). These studies suggested that geostatistical methods provide a promising approach to spatial support change towards a finer scaling mapping rainfall erosivity.

In this paper an attempt has been made to develop a less expensive methodology to predict extreme rainfalls geomorphological impact using the probabilities of exceedance for stormwater erosivity threshold levels. An algorithm for the characterization of this impact, called Erosive Hazard Index (EHI), is developed to be accounted in spatial data exploration. EHI integrate three variables: a dynamic variable which is the erosion index of the current rainstorm and two relative static variables which represent the median of the annual maximum of daily rainfall erosivity, and a dimensionless parameter indicative of the degree ecosystem flexibility. The article is organized as follows. First we shall go into the research methods design on which the EHI algorithm is based. Then we shall demonstrate the method with a case study on an rainstorm dataset. The approach is applied to a test site in Italy Southern Apennines (Benevento province) for control purposes. For this case study we measure and georeference 13 November 1997 storm hydrological data at 39 locations to be combined together into a EHI. Afterwards, a non-parametric geostatistical technique is utilised for erosive hazard spatial uncertainty assessment during single-storm events.

A note on this approach – the issue was regarded by one of the anonymous reviewers that the use of statistics combined with geographical information tools presents a novel approach to the subject.

2. Data Collection and Research Methods Design

The Benevento province is a region of southern Italy, with an areas of approximately 2000 Km^2. Figure 1 shows the location of 39 rain gauges stations used in this study. Annual maximum daily precipitation amount, rainstorm amount and rainfall intensity data have been computed for the period from 1971 to 1997, which was referred by SIMN (1971–1997), Rossi and Villani (1995), and UCEA (1994–1997) datasets, respectively. Data on the hydrogeomorphological events are inferred, instead, from scientific publications (Diodato, 2004b), as well as from technical report (Ispettorato Agricoltura of the Campania Region, 2003).

2.1. Approaches for evaluating the EHI

In EHI modelling, we assume that the river-torrential system has adapted to the natural hydrological regime, and a sudden fluctuation in this regime, especially those exceeding thresholds for an acceptable levels of disturbance, may have disastrous consequences for the mountain environment. The EHI model predicting rainfall impact were derived from modified *intensity pattern* algorithm, utilised by Kuipers

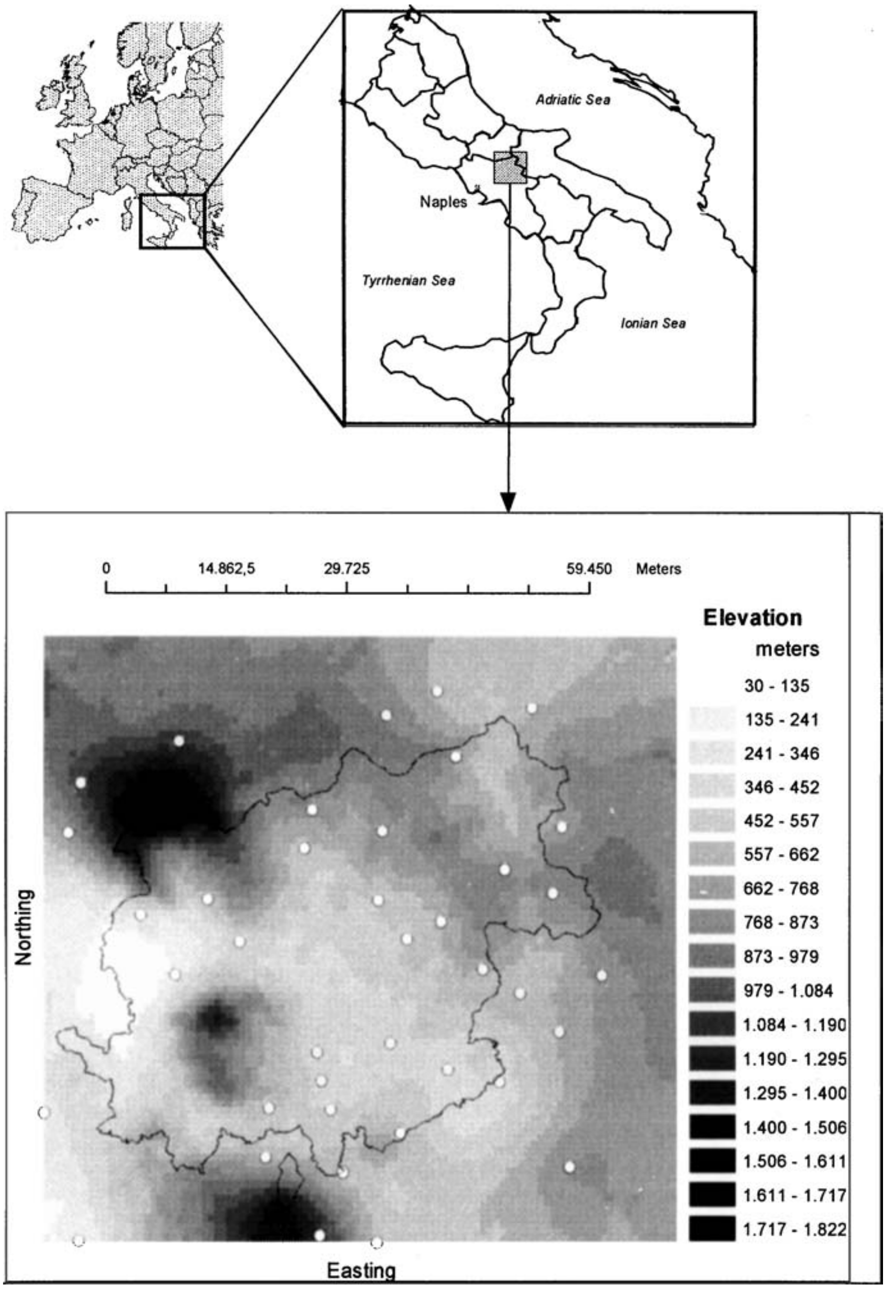

Figure 1. Geographic location of the area under study (above) and morphological characteristics from DEM of the Benevento region (under). The points indicate the 39 rain gauges used in this work.

et al. (2000) in risk analysis of water systems:

$$\mathrm{EHI}_{\mathrm{sto}} = \frac{\mathrm{EI}_{\mathrm{sto}}}{f\left(\mathrm{Med}\left(\mathrm{EI}_{\mathrm{max(d)}}\right)\right)}\left[\ln\left(\frac{\mathrm{EI}_{\mathrm{sto}}}{f\left(\mathrm{Med}\left(\mathrm{EI}_{\mathrm{max(d)}}\right)\right)}\right) - 0 \cdot 1\right] \tag{1}$$

where $\mathrm{EI}_{\mathrm{sto}}$ is the erosion index of the current rainstorm (MJmm $\mathrm{ha}^{-1}\mathrm{h}^{-1}$), that can be subject to large time fluctuation; $\mathrm{Med}(\mathrm{EI}_{\mathrm{max(d)}})$ is the median of the annual maximum of daily rainfall erosion index (MJmm $\mathrm{ha}^{-1}\mathrm{h}^{-1}$) expected on N years, and represents a threshold for natural hydrologic regime; f is a coefficient that explain the degree of local ecosystem flexibility assumed to 1. However, for geomorphological risk assessment f should be evaluate in the order of ecosystem features. In fact, natural land-based ecosystems are generally flexible and capable of absorbing stresses caused by various forms of disturbance (Mendoza *et al*., 2002), including damages from weather events (Evans, 1993; De Luís *et al*., 2001; Ferrero *et al*., 2002), so that $f > 1$. In contrast, landscapes strongly disturbed or degraded (e.g., intensive cropland, indiscriminate urbanisation, landscape post-fire), are commonly little flexible, so that $f < 1$. From the formula (1) it follows that rain aggressiveness impact reaches the critical threshold value 0 when the $\mathrm{EI}_{\mathrm{sto}}$ is close to $\mathrm{Med}(\mathrm{EI}_{\mathrm{max}}(\mathrm{d}))$. It is obvious that for EHI > 0, the hydrogeomorphological system results unstable and the rainfall erosivity-induced hazard is relatively high; conversely, the system results stable for EHI ≤ 0 and hazard is negligible.

2.1.1. *Erosion Index Modelling*

The computation of the single-storm erosion index (EI) is the basis for determining the rainfall factor of RUSLE version (Renard *et al*., 1997) of the well-known empirical model of Universal Soil Loss Equation (Wischmeier and Smith, 1978). The EI is a numerical descriptor of the ability of rainfall to erode soil for a given location (Wischmeier and Smith, 1959). The EI (MJ mm ha^{-1} h^{-1}) index for an event is the product of total storm energy E (MJ ha^{-1}) and maximum 30-min intensity I_{30} (mm h^{-1}): EI $=$ EI_{30}. Since storm energy per unit of rainfall does not vary greatly with rainfall intensity, especially at the higher intensities (Wischmeier and Smith, 1978), total energy E is almost directly proportional to rainfall amount h_e; therefore the EI can be estimated from rainfall amount and maximum 30-min intensity (Foster *et al*., 1982). In this way, an single-storm erosion index (EI) by Bagarello and D'Asaro (1994), developed for Mediterranean area, was utilised to compute EI value at each of the 39 stations:

$$\mathrm{EI} = 0.117 \cdot h_e \cdot (i_{30})^{1.195} \quad r^2 = 0.996 \tag{2}$$

where h_e is the rainstorm amount (mm) and i_{30} is the maximum 30-min intensity (mm h^{-1}).

2.2. Geostatistical indicator approach

For many GIS applications, the user only needs to interpolate point data so that they can be displayed or combined simply with other data. Increasingly, however, GIS are being used to provide data for quantitative models of environmental processes such as climate change, air pollution, land contamination, the diffusion of plants, animals or people (Burrough and McDonnel, 1998). For some models only a deterministic estimate per cell is needed; for others, as in decision making, we need to know the local uncertainty associated at estimate. Such decisions are often based on critical values of pluviometrical indicators. If the estimates are less or more than specified threshold, institutional support may activate land-planning and control measures. But such estimate are usually affected by large uncertainty, arising from sampling, modelling and interpolation, which must be quantified to allow an evaluation of the risk involved in any decision (Buttafuoco *et al.*, 2000). Geostatistics allows to assess such uncertainty through the determination of a conditional cumulative distribution function (ccdf) of the unknown attribute value. We use a non-parametric type of ordinary kriging, called indicator kriging (IK) (Journel, 1983; Isaaks and Srivastava, 1989), because it has the advantage of being resistant to the effects of outlier values, and thus it is useful for analysing skewed datasets, very common in ecological studies to interpolate environmental indicators (Stein *et al.*, 2001). In addition, it is recommended for cases in which the number of experimental data is relatively small and irregularly distributed (Pardo-Igúzquiza, 1998).

In many environmental studies as for assessing weather hazard, the kriging procedure requires the covariance structure of rainfall events in the form of a variogram $2\gamma(\mathbf{h})$, which is a measure of average dissimilarity between data separated by a vector $\mathbf{h}$. The practice of IK involves calculating and modelling indicator variograms $2\gamma_I(\mathbf{h}; z_k)$ (that is, variograms of indicator-transformed data) at one threshold or at a range of cut-offs (Glacken and Blackney, 1998). In other words, $2\gamma_I(\mathbf{h}; z_k)$ measures the transition frequency between two classes of z-values as a function of $\mathbf{h}$ (Goovaerts, 1998). As expected, this variogram quantify the commonly observed relationship between the values of the samples and the samples' proximity.

Consider the values of the random variable Z (Erosive Hazard Index), at n locations $\mathbf{s}_\alpha$, $z(\mathbf{s}_\alpha)$, over the study area. Indicating with F the conditional cumulative distribution function (ccdf) of the variable Z, it results:

$$F(\mathbf{s}_0; z_k \mid (n)) = \text{Prob}\{Z(\mathbf{s}_0) > z_k \mid (n)\} \tag{3}$$

where the notation (n) expresses conditioning to the n data $z(\mathbf{s}_\alpha)$; $\alpha = 1, 2, \ldots, n$, retained in the neighbourhood of $\mathbf{s}_0$. In this approach the probability distribution is regarded as the conditional expectation of the indicator random variable $I(\mathbf{s}_0; z_k)$, given the information (n) data:

$$F(\mathbf{s}_0; z_k \mid (n)) = E\{I(\mathbf{s}_0; z_k) \mid (n)\} \tag{4}$$

with

$$I(\mathbf{s}_0; z_k) = \begin{cases} 1 \rightarrow z(\mathbf{s}_0) > z_k \\ 0 \rightarrow z(\mathbf{s}_0) \leq z_k \end{cases} \tag{5}$$

The least square estimate of the indicator $I(\mathbf{s}_o; z_k)$ is also the least square estimate of its conditional expectation. Thus the ccdf $F(\mathbf{s}_0; z_k \mid (n))$ can be estimated by kriging the indicator $I(\mathbf{s}_0; z_k)$ using binary transformation of data in Equation (5). The ordinary IK estimator is a linear combination of the $n(\mathbf{s}_0)$ indicator $I(\mathbf{s}_\alpha; z_k)$ in the neighbourhood $W(\mathbf{s}_0)$:

$$[I(\mathbf{s}_0; z_k)]^*_{IK} = \sum_{\alpha=1}^{n(\mathbf{s}_o)} \lambda_\alpha(\mathbf{s}_0; z_k) \cdot I(\mathbf{s}_\alpha; z_k) \tag{6}$$

where λ_α $(\mathbf{s}_o; z_k)$ are the weight calculated by solving of the kriging simultaneous equation system (Goovaerts, 1997 p. 294):

$$\begin{cases} \sum_{\beta=1}^{n(\mathbf{s}_o)} \lambda_\beta(\mathbf{s}_0; z_k) \cdot C_I(\mathbf{s}_\alpha - \mathbf{s}_\beta; z_k) + \mu(\mathbf{s}_0; z_k) \\ \quad = C_I(\mathbf{s}_\alpha - \mathbf{s}_0; z_k) \quad \alpha = 1, \ldots, n(\mathbf{s}_0) \\ \sum_{\beta=1}^{n(\mathbf{s}_0)} \lambda_\beta(\mathbf{s}_0; z_k) = 1 \end{cases} \tag{7}$$

with $C_I(\mathbf{s}_\alpha - \mathbf{s}_o; z_k)$ being the covariance function of the indicator $I(\mathbf{s}_0; z_k)$ at threshold z_k. For this case study, it was assumed that areas where EHI was above $z_k = 0$ had been affected by geomorphological instability. Availability of EHI ccdf model $F(\mathbf{s}_0; z_k|(n))$ for each location s_0 within the study area allows grid layer of: the susceptibility $\alpha(\mathbf{s}_0)$ of declaring a location 'hazard' by erosion on the basis of the estimate $I(\mathbf{s}_0; z_k)^*$ when actually $Z(\mathbf{s}_0) > z_k$. Each component spatial and probability map based on thresholds of EHI determined in kriging, was estimated with over 3600 (1000 × 1000 m) cells. The estimates of the spatial components and the exceeding threshold probabilities of these environmental parameters, as well as the kriging performance, were made within Geostatistical Analyst modules implemented in ArcGis 8.1–ESRI software (Johnston *et al.*, 2001).

2.3. Cross-validation method

The performance of IK algorithm, was assessed using cross validation (Isaaks and Srivastava, 1989). The idea deals in re-estimating EHI data at rain gauge locations after removing, a turn, one EHI datum from the dataset. The difference between the estimated indicator value and the corresponding measured one is the experimental error. Thus, repeating this estimation for the number of the experimental data $n = 39$, the cross-validation statistics may be calculated, as Mean Errors (ME), Root

Mean Square Errors (RMSE), Average Standard Errors (ASE), Mean Standard Errors (MSE) and Root-Mean-Square Standardized Error (RMSSE). ME should be close to 0. RMSE and ASE are indices that represent the variability prediction; while RMSSE compare the error variance with same theoretical variance, such as kriging variance. Therefore, it should be close to 1. The final interpolated and actual values are compared, and the model that yields the most accurate predictions is retained.

3. Case Study

To illustrate the applicability of the proposed methodology, a reference classification are constructed from EHI from rainstorm event on November 13, 1997 in Benevento province (Southern Italy). The Benevento province is a topographically complex region of the central Mediterranean (southern Italy), with an extension of approximately 4000 km^2 (Figure 1). Due of the Mediterranean area, geographical features (i.e., Alps and Apennines chain, the Plain and Sea) and their effects on the mesoscale circulation generates a variety of precipitation (Meneguzzo *et al*., 1996; Paolucci *et al*., 1999). In the cold season, the rain may be principally due to fronts associated to Mediterranean cyclone. The airflow activity is particularly important on the surrounding Apennines chain, where the lifting of the air masses causes frequent orographic precipitation. So that there the rainfall is abundant in the early winter and the spring, when also the thermic sea – atmosphere contrast is more marked. In Benevento, river-torrential landscape mean annual rainfall totals are of the order of 700–900 mm y^{-1}. However, interannual variability is considerable, e.g., totals of 483 mm in 1945 and 1876 mm in 1915 (Diodato, 2002).

3.1. Rainstorm types: observational approach

Based on the concept of geomorphological effectiveness (after Molnar *et al*., 2002), three different types of rainstorm can be defined: (a) rainstorms that have extraordinary intensity (80–140 mm h^{-1}), but have very short duration, typical of afternoons in late spring or during the summer period. Examples of these types are heavy showers or thunderstorms commonly localised causing surface erosion by overland flow in the form of rill and gully erosion with remarkable mass movements on the torrential landscape, as happened recently on May and July 1999, May and June 2000, 2003; (b) rainstorms that have high intensity (20–80 mm h^{-1}), and extension, and are of more longer duration, exhibiting relevant geomorphological effectiveness. They are associated with a high-erosion rate, floods in form of flash-floods, landslides and dramatic changes in channel shape and form, as happened on September 1857, October 1875, September and November 1889, October 1899, 1949 and 1961, November 1985 and 1997 (Diodato, 1999); (c) rainstorms of long duration but low intensity (5–20 mm h^{-1}), sometimes with snowmelts. They can be associated to floods commonly occurring in large lowland Tammaro and Calore river of Benevento region, and landslides, as happened on January 1895 and 1900, February 1905 and 1938, October 1961, December 1968 and January 2003.

The total rainfall recorded on 13 November 1997 from agrometeorological-based station (Monte Pino Research Observatory) located in cropland of the Benevento district was 111 mm, 86 mm of which fell in 3 h. The analysis of historical rainfall data in this area using the Gumbel method, referred to as 3 h rainfall, shows that this rainfall of 86 mm has a return period of 20 years. The energy of the storm in form the erosion index reached a value of 933 MJmm $ha^{-1}h^{-1}$. This value is about equal to annual average value for this area, which gives an idea of the very high erosive and overland flow potentiality of this storm.

3.2. Distribution of the Data

The first step in the environmental impact assessment within a geostatistical study is a preliminary knowledge of the phenomenon features and data distribution. Data analysis and interpretation cannot be completely automated, particularly when making crucial modelling choices (Kitanidis, 1997). It was quite obvious from the start that the 39-sample pluviometrical parameters had a skewed distribution (Figure 2). Ordinary kriging is quite robust and so there is some potential for applying ordinary kriging. Nevertheless, probability map for ordinary kriging requires that data follow

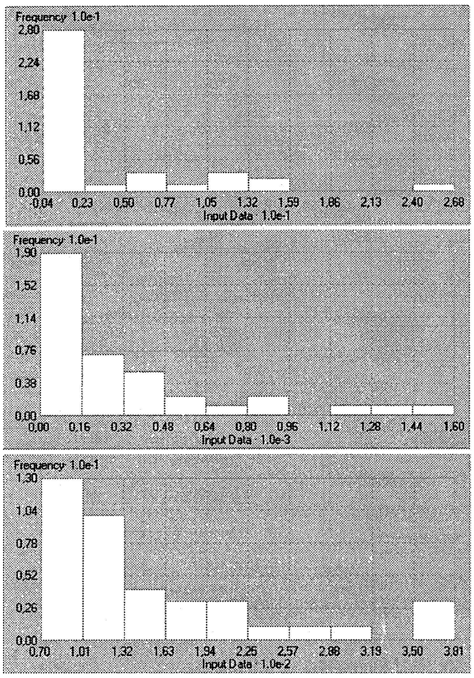

EHI Statistics

Count	: 39	Skewness	: 2,1142
Min	: -0,41	Kurtosis	: 7,5087
Max	: 26,76	1-st Quartile	: -0,3025
Mean	: 3,3238	Median	: 0,5
Std. Dev.	: 5,9884	3-rd Quartile	: 4,945

EI_{sto} Statistics

Count	: 39	Skewness	: 1,7289
Min	: 4	Kurtosis	: 5,2565
Max	: 1602	1-st Quartile	: 53,75
Mean	: 323,38	Median	: 167
Std. Dev.	: 404,31	3-rd Quartile	: 448,75

Med($EI_{max(d)}$) Statistics

Count	: 39	Skewness	: 1,4128
Min	: 70	Kurtosis	: 4,0731
Max	: 381	1-st Quartile	: 100
Mean	: 153,03	Median	: 120
Std. Dev.	: 83,922	3-rd Quartile	: 188,75

Figure 2. Histograms EHI, EI_{sto} and $M(EI_{max(d)})$ data (left) and their respective statistics (right).

a multivariate normal distribution. Also disjunctive kriging (Rivoirard, 1994) at our case because the assumptions of bivariate normal distribution (Chilès and Delfiner, 1999; by Johnston *et al.*, 2001) is not appropriate. An alternative approach, and the one which we adopted, is IK. Since IK works by decomposing the variable of interest into several binary variables, and in doing so decomposing the univariate distribution function (histogram) into several classes, the dependence on a normal distribution disappears (Journel, 1983). It is mainly for this reason that we decided to adopt ordinary IK.

3.3. Spatial structural modelling

A model of coregionalization was fitted using an iterative procedure developed by Johnston *et al.* (2001), and composed of two stages. Stage 1 begins by assuming an isotropic model, and it executes a first run of the empirical semivariogram model. The semivariogram lag-distance measures the average degree of dissimilarity between an unsampled value $z(\mathbf{s})$ and nearby data values. With Stage 2 any parameter, such as number of *lag* (assumed equal 7), or *lag* size $\mathbf{h}$ (assumed equal 5000 meters), *range* a, *nugget* C_0 and *partial sill* C_1 is calibrated interactively (Table I). Also at this stage it has been assumed a isotropic model. However, this is critical subject as it was not possible to verify the contrary because of small sample size. In this way, Figure 3 shows the experimental semivariograms computed from the 39 data of EHI predicted for November 13 1997, with hole effect permissible models

TABLE I
Parameters of indicator semivariograms for Erosive Hazard Index data

EHI thresholds	Nugget effect	Structure		Model
		Partial sill	Range (m)	
EHI = 0	0.04702	0.19800	34821	Hole effect
EHI = 4.95	0.07000	0.15598	30000	Hole effect

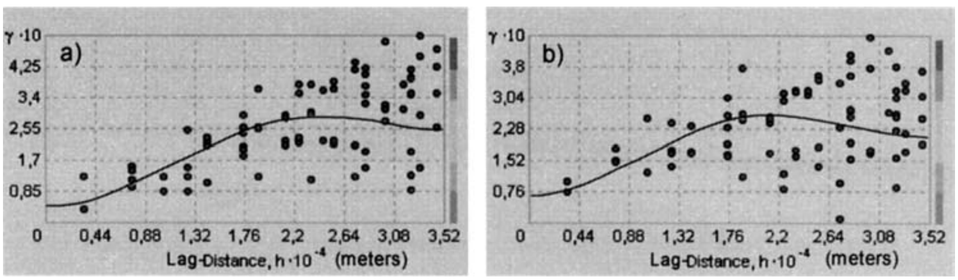

Figure 3. Model of regionalization (solide curves) for EHI > 0 (a) and EHI > 4.95 (b).

fitted. Semivariogram values increase with the separation distance, reflecting the assumption that rainfall impact data nearby tend to be more similar than data that are farther apart. The semivariogram reaches a maximum at 30000–34000 m before dipping and fluctuating around a sill value. Unidirectional semivariograms were modelled as a combination of two distinct spatial structures: nugget variance and a hole effect structure:

$$\gamma(\mathbf{h}) = \begin{cases} C_0 \cdot \text{Nugget} & \mathbf{h} = 0 \\ C_0 \cdot \text{Nugget} + C_1 \cdot \text{Hole effect}(|\mathbf{h}|, a) & \mathbf{h} > 0 \end{cases} \tag{8}$$

where HoleEffect($|\mathbf{h}|$, a) represent a dimensional Hole effect variogram of unit sill with practical ranges given by the circle with $a =$ range. The function Hole effect model equal to (Johnston *et al.*, 2001):

$$\left\{\frac{1 - \sin((2\Pi|\mathbf{h}|)/a)}{\sin((2\Pi|\mathbf{h}|)/a)}\right\}.$$

Ideally the value of the semivariogram should be zero when the separation vector $\mathbf{h}$ is zero; in the case study this is not true principally because measurement error exists, and secondary because the EHI spatial variability at distance $<$5000 meters is unknown.

3.4. Spatial pattern of estimation and EHI classification

Figure 4 shows indicator kriged probability map on the basis of the threshold of EHI 1000 $\times$ 1000 m grid. The map indicate that the phenomenon accounted by IK is not smooth (i.e., EHI values change strongly with the distance). In this respect the non-linear semivariogram with hole effect and nugget effect was selected as the base model for calculations, so that variogram models estimations which differ significantly from the known value even at short distances. The so-called hole effect model typically reflects pseudo-periodic or cyclic phenomena (Journel and Huijbregts, 1978). Here, the hole effect relates to the existence of three mountains 2000 m apart, aligned in the north to south direction at western of the Benevento district (Figure 1), which creates one high-valued area in the intense-rainfall bands. The impact rainfall bands are focused on the small-scale topography, oriented south – north, composed of a succession of ridges and penetrating valleys (Figure 4b).

In addition, GIS was used mainly used to add a group layer. So that a layer that delimits the extent of the geomorphological processes observed on 13 November 1997, was overlaid on the kriging maps which find the areas probably subjected to erosional soil degradation ($p > 0.5$) for exceeding the threshold EHI = 0 (Figure 5a), and for EHI = 4.95 falling above the 75th quantile (Figure 5b). Both maps according with observation, especially those of Figure 5a, which accurately

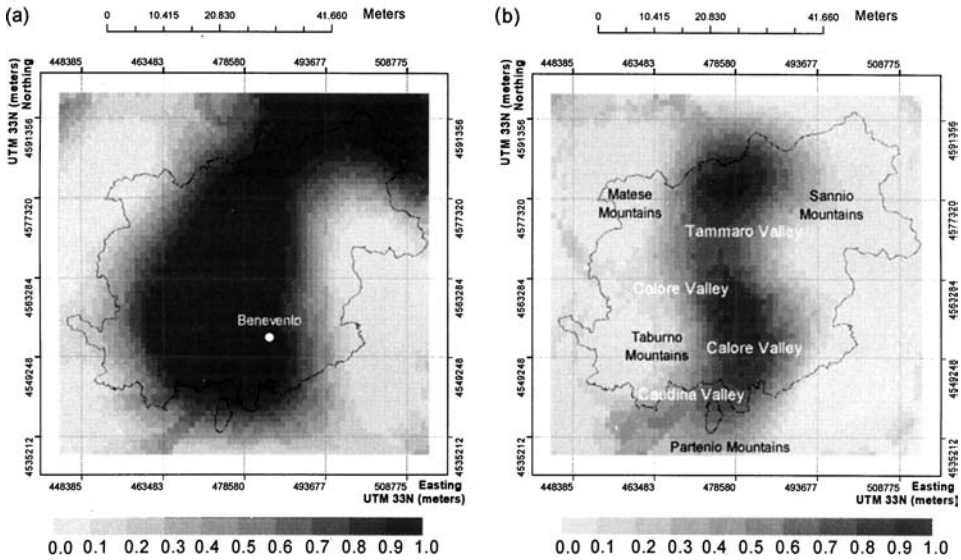

Figure 4. Kriged probability maps of the EHI > 0 (a) and EHI > 4.95 (b) for rainstorm event on 13 November 1997.

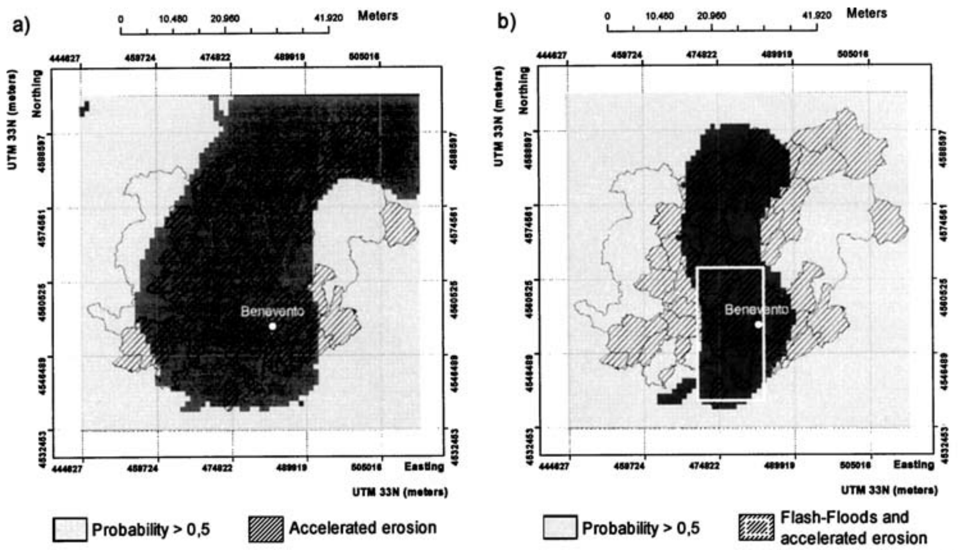

Figure 5. Kriged maps with high probabilities (>0.5) of the EHI > 0 (a) and EHI > 4.95 (b) for rainstorm event on 13 November 1997.

predict the areas interested from soil erosion processes. By field observations, in fact, severe erosive processes covering large areas of sloping land, flash-floods with river erosion was surveyed in the Benevento south province across the main town, and in some zones at north.

TABLE II
Prediction errors among actual EHI and the indicator prediction of kriging

Prediction standard error	EHI = 0	EHI = 4.95
Mean	0.0395	0.0510
Root-mean-square	0.3229	0.3850
Average-standard-error	0.3365	0.3901
Mean-standardized	0.0564	0.1110
Root-mean-square-standardized	0.9620	1.0470

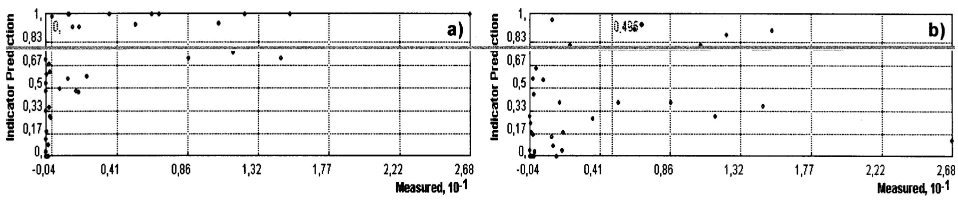

Figure 6. Scatter diagram among measured erosive hazard index and the indicator prediction of kriging for the EHI > 0 (a) and EHI > 4.95 (b).

3.5. Cross-validation results

The cross-validation results are displayed in Table II. Mean equal to 0.039–0.051, showing lack of systematic error. Since Root-Mean-Square is close to the Average-Standard-Errors, Mean is correctly assessing the variability in prediction. Also kriging variance result correctly assessing because Root-Mean-Square-Standardized is close to 1. Other criteria of comparison are given in scatter diagram of Figure 6, where the predicted indicators values versus the measured values of rainfall are represented, confirming the performance in the statistical sense.

3.6. Error assessment

At this preliminary stage, the validation was done by local experts by qualitative assessment based on their experience. However, at such a scale, it is necessary to use error assessment and validation procedures. Other ways to validate can be identified. (i) A first approach would be to compare the results from study like this with actual soil erosion risk derived by experimental measure sediment done on small catchments. (ii) A second approach would compare the results from models simulations approach (Beeson *et al.*, 2001) that provides a spatially explicit assessment of impacts on overland flow at sub-regional scale.

4. Conclusions

Because the soil erosion risk assessment is often founded on long-term average precipitation patterns, knowledge in soil erosion hazard – rainfall erosivity typically is incomplete. Alternative or integrative methods can be used to increase understanding of hazard at any given site during single rainstorm event. GIS using non-parametric geostatistical techniques provide a means to help characterize the spatial distribution of the rainstorm impact through spatial mapping of a EHI and therefore provide an economical and preliminary approach in erosional soil degradation assessment. Indicator kriging is a particularly promising modelling technique in that the resulting model defines the probability of exceedance of a given threshold for rainfall aggressiveness. The method is recommended for cases in which the experimental data is skewed and irregularly distributed. Therefore, the association between storm type and stage of the wet season suggests that covariance structure of daily rainfall might change through the season. In this work we only deal with the single storm analysis but future research comprises to develop models including the statistic of the climatic extremes erosive hazard.

Acknowledgements

I gratefully acknowledge the two anonymous reviewers for providing helpful suggestions and Lorenzo Borselli (Ph.D. car of Research Institute for the Hydrogeological Protection CNR – IRPI, Italy) for editing of manuscript.

References

Abel, A., Michael, A., Zartl, A. and Werner, F.: 2000, 'Impact of erosion-transported overburden dump materials on water quality in Lake Cospuden evolved from a former open cast lignite mine south of Leipzig, Germany', *Environ. Geol.* **39**(6), 683–688.

Atkinson P. M. and Lloyd C. D.: 1998, 'Mapping precipitation in Switzerland with ordinary and indicator kriging', *J. Geogr. Inform. Decision Anal.* **2**(2), 65–76.

Alpert, P., Ben-Gai, T., Baharad, A., Benjamini, Y., Yekutieli, D., Colacino, M., Diodato, L., Ramis, C., Homar, V., Romero, R., Michaelides, S. and Manes, A.: 2002, 'The paradoxical increase of Mediterranean extreme daily rainfall in spite of decrease in total values', *Geophys. Res. Lett.* **29**(11), 135–154.

Al-Sheriadeh, M. S. and Al-Harndan, A. Z.: 1997, 'Erosion risk assessment and sediment yield production of the King Talal Watershed, Jordan', *Environ. Geol.* **37**(3), 234–242.

Arshad, M. A. and Martin, S.: 2002, 'Identifying critical limits for soil quality indicators in agro-ecosystems', *Agric. Ecosyst. Environ.* **88**, 153–160.

Bagarello, V. and D'Asaro, F.: 1994, 'Estimating single storm erosion index', *Trans. Am. Soc. Agric. Eng. ASAE* **3**, 785–791.

Balling Jr, R. and Cerveny, R. S.: 2003, 'Compilation and discussion of trends in severe storms in the United States: Popular perception vs. climate reality', *Nat. Hazards* **29**(2), 103–112.

Bazzoffi, P., Pellegrini, S., Chisci, G., Papini, R. and Scagnozzi, A.: 1997, 'Erosione e deflussi a scala parcellare e di bacino in suoli argillosi a diversa utilizzazione nella val d'Era', *Agric. Ric.* **170**, 5–20.

Beeson, P. C., Artens, S. and Breshears, D. D.: 2001, Simulating overland flow following wildfire: Mapping vulnerability to landscape disturbance', *Hydrolog. Processes* **15**, 2917–2930.

Bell, J. L., Sloan, L. C. and Snyder, M. A.: 2004, Regional changes in extreme climatic events: A future climate scenario. *J. Climate* **17**, 81–87.

Brunetti, M., Maugeri, M. and Nanni, T.: 2001, 'Changes in total precipitation, rainy days and extreme events in Northeastern Italy', *Int. J. Climatol.* **21**, 861–871.

Bryant, E.: 1991, *Natural Hazard,* Cambridge University Press, New York, 285 pp.

Burrough, P. A. and McDonnell, R. A.: 1998, *Principles of Geographical Information Systems,* Oxford University Press, New York, pp. 98–161.

Buttafuoco, G., Castrignanò, A. and Stelluti, M.: 2000, 'Accounting for Local Uncertainty in Agricultural Management Decision Making', in: *7th ICCTA International Congress for Computer Technology in Agriculture,* 15–18 November 1998, Florence, pp. 510–517.

Camara Belmonte, A. and Segura Beltrán, F.: 2001, 'Flood events in Mediterranean ephemeral stream (ramblas) in Valencia region, Spain', *Catena* **45**(3), 229–249.

Cheng, K. S., Wei, C., Cheng, Y. B. and Yeh, H. C.: 2003, 'Effect of spatial variation characteristics on contouring of design storm depth', *Hydrolog. Processes* **17**(9), 1755–1769.

Chilès, J. P. and Delfiner, P.: 1999, *Geostatistics Modeling Spatial Uncertainty,* Wiley, New York, 695 pp.

Conedera, M., Peter, L., Marxer, P., Forster, F., Rickenmann, D. and Re, L.: 2003, 'Consequences of forest fires on the hydrogeological response of mountain catchments: A case study of the Riale Buffaga, Ticino, Switzerland', *Earth Surface Processes Landforms* **28**, 117–129.

Cooke, R. U. and Doornkamp, J. C.: 1990, *Geomorphology in Environmental Management,* Clarendon Press, Oxford, p. 79.

Coppus, R. and Imeson, A. C.: 2002, 'Extreme events controlling erosion and sediment transport in a semi-arid sub-Andean Valley', *Earth Surface Processes Landforms* **27**, 1365–1375.

Cox, C. and Madramootoo, C.: 1998, 'Application of geographic information systems in watershed management planning in St. Lucia', *Computer Electron. Agric.* **20**, 229–250.

De Luís, M., García-Cano, M. F., Cortina, J., Raventós, J., Gonzáles-Hidalgo, J. C. and Sánchez, J. R.: 2001, 'Climatic trends, disturbances and short-term vegetation dynamics in a Mediterranean shrubland', *Forest Ecol. Manage.* **147**, 25–37.

de Santos Loureiro, N. and de Azevedo Coutinho, M.: 1995, 'Rainfall changes and rainfall erosivity increase in the Algarve (Portugal)', *Catena* **24**, 55–67.

Diodato, N.: 1999, 'Ricostruzione storica di eventi naturali estremi a carettere idrometeorologico nel Sannio beneventano dal Medioevo al 1998', *Bollettino Geofis.* **22** (3/4), 5–39.

Diodato, N.: 2002, 'Ricostruzione storica di dei rilevamenti pluviometrici nell'Italia peninsulare: il caso dell'Osservatorio Meteorologico di Benevento – Centro Storico (1869–1999)', *Bollettino Geofis.* **25**(1/2), 27–44.

Diodato, N.: 2004a, 'Estimate RUSLE's rainfall factor in the part of Italy with a Mediterranean rainfall regime', *Hydrol. Earth Syst. Sci.* **8**(1),103–107.

Diodato, N.: 2004b, 'Local models for rainstorm-induced hazard analysis on Mediterranean river-torrential geomorphological systems', *Nat. Hazard Earth Syst. Sci.* **4**, 389–397.

Evans, R.: 1993, 'Sensivity of the British Landscape to Erosion', in: D. S. G. Thomas and R. J. Allison (eds), *Lanscape Sensivity*, Wiley, Chichester, pp. 189–210.

Ferrero, A., Lisa, L., Parena, S. and Sudiro, L.: 2002, 'Run-off and Soil Erosion from Tilled and Controlled Grass-Covered Vineyards in a Hillside Catchment', *Report presented to ERC and Northern European FRIEND Project 5th Conference*, Demanovska dolina, Slovakia, 4 pp.

Foster, G. R., Lombardi, F. and Moldenhauer, W. C.: 1982, 'Evaluation of rainfall-runoff erosivity factors for individual storms', *Trans. Am. Soc. Agric. Eng. ASAE* **25**(1), 124–129.

Gardner, R. A. M. and Gerrard, A. J.: 2003, 'Runoff and soil erosion on cultivated rainfed terraces in the Middle Hills of Nepal', *Appl. Geogr.* **23**, 23–45.

Glacken, I. and Blackney, P.: 1998, 'A Practitioners Implementation of Indicator Kriging', in: *Proceedings of the Symposium on Beyond Ordinary Kriging*, 30 October 1998, Perth Western, Australia, pp. 26–39.

Goovaerts, P.: 1997, *Geostatistics for Natural Resources Evaluation*, Oxford University Press, New York, 483 pp.

Goovaerts, P.: 1998, 'Geostatistical tools for characterizing the spatial variability of microbiological and physico-chemical soil properties', *Biol. Fertil Soils* **27**, 315–334.

Goovaerts, P.: 1999, 'Using elevation to aid the geostatistical mapping of rainfall erosivity', *Catena* **34**, 227–242.

Isaaks, E. H. and Srivastava, R. M.: 1989, *An Introduction to Applied Geostatistic,* Oxford University Press, New York, 561 pp.

Ispettorato Agricoltura of the Campania Region: 2003, Technical Reports, documents unpublished.

Journel, A. G.: 1983, 'Non-parametric estimation of spatial distributions', *Math. Geol.* **15**, 445–468.

Journel, A. G. and Huijbregts, C. J.: 1978, *Mining Geostatistics*, Academic Press, London.

Hooke, J. M. and Mant, J. M.: 2000, 'Geomorphological impacts of a flood event on ephemeral channels in SE Spain', *Geomorphology* **34** (3, 4), 163–180.

Jansson, M. B.: 1982, Land Erosion by Water in Different Climates, *UNGI Rapport, 57.* Uppsala University, Department of Physical Geography, 150 pp.

Johnston, K., Ver Hoef, J. M., Krivoruchko, K. and Lucas N.: 2001, *Using ArcGis Geostatistical Analyst*, ESRI, 300 pp.

Kitanidis, P. K.: 1997, *Introduction to Geostatistics: Applications to Hydrogeology*, Cambridge University Press, New York, 246 pp.

Krishnaswamy, K., Richter, D. D., Halpin, P. N. and Hofmockel, M. S.: 2001, 'Spatial patterns of suspended sediment yields in a humid tropical watershed in Costa Rica', *Hydrolog. Processes* **15**, 2237–2257.

Kuipers, F., Kok, M. and Vermeulen, C. J. M.: 2000, 'Modelling of Extreme Precipitation Events in Risk Analysis of Water System', in *Report Presented at the 8th International Symposium on Stochastic Hydraulics*, 25–28 July 2000, Beijing, pp. 10.

Lal, R.: 1997, 'Degradation and resilience of soils', *Phil. Trans. Royal Soc. London* B**352**, 997–1010.

Larson, W. E., Lindstrom, M. J. and Schumacher, T. E.: 1997, 'The role of severe storms in soil erosion: A problem needing consideration', *J. Soil Water Conserv.* **52**(2), 90–95.

Le Bissonnais, Y., Montier, C., Jamagne, M., Daroussin, J. and King, D.: 2002, 'Mapping erosion risk for cultivated soil in France', *Catena* **46**, 207–220.

Lin, C. Y., Lin, W. T. and Chou, W. C.: 2002, 'Soil erosion prediction and sediment yield estimation: The Taiwan experience', *Soil Tillage Res.* **68**, 143–152.

Mati, B. M., Morgan, R. P. C., Gichuki, F. N., Quinton, J. N., Brewer, T. R. and Liniger, H. P.: 2000, 'Assessment of erosion hazard with the USLE and GIS: A case study of the Upper Ewaso Ng'iro North basin of Kenya', *J. Am. Geol.* **2**(1), 1–8.

Martìnez-Casasnovas, J. A., Ramos, M. C. and Ribes-Dasi, M.: 2002, 'Soil erosion caused by extreme rainfall events: mapping and quantification in agricultural plots from very detailed digital elevation models', *Geoderma* **105**, 125–140.

Mazzarela, A., Tranfaglia, G. and Di Donna, G.: 1999, 'Il contributo della geometria frattale alla stima del deficit risolutivo di una rete di pluviometri e del rischio di piogge intense', *Bollettino Geofis.* **22** (3/4), 61–71.

Mendoza, G. A., Anderson, A. B. and Gertner, G. Z.: 2002, 'Integrating multi-criteria analysis and GIS for land condition assessment: Part I–Evaluation and restoration of military training areas', *J. Geogr. Inform. Decision Anal.* **6**(1), 1–16.

Meneguzzo, F., Giarola, S., Grippa, G. and Gozzini, B.: 1996, 'Mesoscale operational rainfall forecasts in north-western Tuscany', *Bollettino Geofis.* **19**(3/4), 39–55.

Mikhailova, E. A., Bryant, R. B., Schwager, S. J. and Smith, S. D.: 1997, 'Predicting rainfall erosivity in Honduras', *Soil Sci. Soc. Am. J.* **61**, 273–279.

Mitasova, H., Hofierka, J., Zlocha, M. and Iverson, L. R.: 1996, 'Modeling topographic potential for erosion and deposition using GIS', *Int. J. Geogr. Inform. Sci.* **10**(5), 629–641.

Molnar, P., Burlando, P. and Ruf, W.: 2002, 'Integrated catchment assessment of riverine landscape dynamics', *Aquatic Sci.* **64**, 129–140.

Morgan, R. P. C.: 1995, *Soil Erosion and Conservation*, Longman, Essex, p. 298.

Mulligan, M.: 1998, 'Modelling the geomorphological impact of climatic variability and extreme events in a semiarid environment', *Geomorphol.* **24**(1), 59–78.

Paolucci, T., Bernardini, L., Ferretti, R. and Visconti, G.: 1999, 'Flood forecast a hight resolution limited area model', *Il Nuovo Cimento* **22C**(5), 727–736.

Pardo-Igúzquiza, E.: 1998, 'Comparison of geostatistical methods for estimating the areal average climatological rainfall mean using data on precipitation and topography', *Int. J. Climatol.* **18**, 1031–1047.

Prudhomme, C. and Reed, D. W.: 1999, 'Mapping extreme rainfall in a mountainous region using geostatistical techniques: A case study in Scotland', *Int. J. Climatol.* **19**, 1337–1356.

Ramírez, J. A. and Finnerty, B.: 1996, 'Precipitation and water-table effects on agricultural production', *J. Irrigat. Drainage Eng.* **122**, 164–171.

Ramos, M. C. and Mulligan, M.: 2003, 'Impacts of climate variability and extreme events on soil hydrological processes', *Geophys. Res.* **5**, 92–115.

Renard, K. G., Foster, G. R., Weesies, G. A., McCool, D. K. and Yoder, D. C.: 1997, *Predicting Soil Erosion by Water: A Guide to Conservation Planning with the Revised Universal Soil Loss Equation (RUSLE)*, USDA, Agricultural Handbook, 703, 384 pp.

Renschler, C. S., Mannaerts, C. and Diekkruger, B.: 1999, 'Evaluating spatial and temporal variability in soil erosion risk-rainfall erosivity and soil loss ratios in Andalusia, Spain', *Catena* **34** (3/4), 209–225.

Renschler, C. and Harbor, J.: 2002, 'Soil erosion assessment tools from point to regional scales the role of geomorphologists in land management research and implementation', *Geomorphology* **47**(2–4), 189–209.

Rivoirard, J.: 1994, *Introduction to Disjunctive Kriging and non-linear Geostatistics,* Clarendon Press, Oxford, 180 pp.

Rossi, F. and Villani, P.: 1995, *Valutazione Delle Piene in Campania. Allegato: Tabelle Pluviometriche*, CNR–GNDCI, Presidenza del Consiglio dei Ministri, Dipartimento della Protezione Civile.

SIMN: 1971–1997, *Annali Idrologici*. Servizio Idrografico e Mareografico Nazionale Italiano.

Shi, Z. H., Cai, C. F., Ding, S. W., Li, Z. X., Wang, T. W. and Sun, Z. C.: 2002, 'Assessment of Erosion Risk with the Rusle and GIS in the Middle and Lower Reaches of Hanjiang River', in: *12th ISCO Conference*, Beijing, 73–78.

Singh, R. B. and Sen Roy, S.: 2002, 'Climate Variability and Hydrological Extremes in a Himalayan Catchment', in: *ERB and Northern European FRIEND Project 5 Conference*, Demänovská dolina, Slovakia, pp. 32–35.

Steer, A.: 1998, 'Making development sustainable', *Adv. Geo-Ecological* **31**, 857–865.

Stein, A., Riley, J. and Halberg, N.: 2001, 'Issues of scale for environmental indicators', *Agric. Ecosyst. Environ.* **87**(2), 215–232.

Trenberth, K. E.: 1999, ‘Conceptual framework for changes of extremes of the hydrological cycle with climate change’, *Clim. Change* **42**(1), 327–339.

Thornes, J. B. and Alcantára-Ayala, I.: 1998, ‘Modelling mass failure in a Mediterranean mountain environment: Climatic, geological, topographical and erosional controls’, *Geomorphology* **24**(1), 87–100.

UCEA–*Bollettino Agrometeorologico Nazionale:* 1994–1997, Ministero Risorse Agricole e Forestali, Roma.

Van der Knijff, J. M., Jones, R. J. A. and Montanarella, L.: 2000, Soil Erosion Risk Assessment in Italy, *European Commission–Report European Soil Bureau*; 52 pp.

Wainwright, J.: 1996, ‘Infiltration, runoff and erosion characteristics of agricultural land in extreme storm events, SE France’, *Catena* **26**(1, 2), 27–47.

Wang, G., Gertner, G., Singh V., Shinkareva, S., Parysow, P. and Anderson A. 2002, ‘Spatial and temporal prediction and uncertainty of soil loss using the revised universal soil loss equation: A case study of the rainfall-runoff erosivity *R* factor’, *Ecologic. Modelling* **153**(1/2), 143–155.

Wischmeier, W. H. and Smith, D. D.: 1959, ‘A rainfall erosion index for a universal soil loss equation’, *Soil Sci Soc. Am. Proc.* **23**(3), 246–249.

Wischmeier, W. H. and Smith, D. D.: 1978, *Predicting Rainfall Erosion Losses*, Admin. U.S. Department of Agriculture, Washington, D.C., Agriculture Handbook. Sci. And Educ. 357, 58 p.